Görtler vortices in the Rayleigh layer on an impulsively started cylinder

Sharon O. MacKerrell[a)]
School of Mathematics and Statistics, University of Birmingham, Birmingham B15 2TT, United Kingdom

P. J. Blennerhassett[b)] and Andrew P. Bassom[c)]
School of Mathematics, University of New South Wales, Sydney NSW 2052, Australia

(Received 24 September 2001; accepted 24 May 2002; published 25 July 2002)

Centripetal instabilities in two flows involving time-dependent Rayleigh layers on a rotating circular cylinder are examined. In one case we consider the stability of the flow induced in an infinite expanse of quiescent fluid when the cylinder is impulsively given a constant angular velocity; in the other problem the angular velocity increases as the square root of time so that the undisturbed flow has a constant wall shear. For both situations linear neutral stability curves for vortex motions are calculated by quasi-steady (or frozen-time) methods, with these results justified, where possible, by Wentzel–Kramers–Brillouin techniques. The topology of the neutral curve for the ramped angular velocity configuration allows a rigorous description of small wavelength, weakly and fully nonlinear vortex structures to be obtained. Our results are compared with the equivalent cases that arise in the study of unsteady thermal Rayleigh layers induced by the sudden heating of a horizontal flat plate. © *2002 American Institute of Physics.* [DOI: 10.1063/1.1495869]

I. INTRODUCTION

The stability of time-dependent Couette flow has been investigated extensively using both experimental[1–3] and theoretical[4–8] techniques. For the particular case of impulsively started Couette flow good agreement has been obtained between experimental results[1] and theoretical predictions[5] for the initiation of Taylor vortices in the flow. Other time-dependent aspects of the now classical Taylor vortex flow have also been investigated[2–4] providing a wide range of information on the evolution of vortex motion in centripetally unstable time-varying flows. Despite the importance of these recent experimental developments, the problems investigated here concern more fundamental properties of the linear theory neutral stability curves for two flows related to the time-dependent Taylor vortex flow. Our primary aim is to delineate the regions of parameter space where the commonly used quasi-steady approximation can be mathematically justified, and from there construct mathematically valid solutions for the nonlinear development of the time-dependent flow. In one case we consider the stability of the flow generated in an infinite expanse of quiescent fluid when a circular cylinder is impulsively given a constant angular velocity and, in the other, the flow when the angular velocity is proportional to the square root of time. This latter situation causes the undisturbed flow to have a constant wall shear stress, and will be referred to as the impulsive shear case, while the previous configuration is the impulsively started flow. Both of the above flows are unstable to small amplitude toroidal vortices, periodic along the length of the cylinder.

Given the well-known analogy between thermal and centripetal instability in steady flows, the unsteady boundary layers, or Rayleigh layers, described above might also be expected to have similar stability properties to thermal Rayleigh layers generated by impulsively heating a horizontal flat plate in a quiescent fluid. Unlike the impulsive Couette problem, the time-dependent thermal problems have been subject to continuing experimental[9] and theoretical[9,10] investigation, possibly due to persistent differences between observations and predictions. A secondary aim of the work presented is to demonstrate the differences in the structure of the linear stability properties of these classes of unsteady flows.

As the flows under consideration are centripetally unstable some Taylor number (or Görtler number) might be expected as the parameter governing the stability of the motion. However, the problems as sketched above have only the cylinder radius as the imposed geometrical length scale and hence a Taylor number cannot be defined from the data of the problem. For both of the flows considered it is possible to anticipate a quasi-steady, or ''frozen-time,'' stability analysis and use a ''Rayleigh layer thickness'' as the length scale for the resulting vortex motion. This would lead to linear stability equations analogous to those of the standard steady Taylor–Görtler vortex problem.[8] For the approach adopted here, only the given physical data in the problem are used to make the governing equations nondimensional, so that the independent variable *time* becomes the fundamental quantity characterizing the stability of the flow. Neitzel[7] also reported the results of his numerical solutions in terms of time to instability.

The use of time as the variable determining instability uncovers a fundamental difference in the stability character-

[a)]Electronic mail: S.O.MacKerrell@bham.ac.uk
[b)]Electronic mail: P.Blennerhassett@unsw.edu.au
[c)]Permanent address: School of Mathematical Sciences, University of Exeter, North Park Road, Exeter, Devon EX4 4QE, U.K. Electronic mail: A.P.Bassom@ex.ac.uk

istics of the impulsively started flow and the impulsive shear case. For example, as time increases in the impulsively started flow the width of the band of unstable axial wave numbers shrinks to zero, while, as time becomes large, the constant shear case becomes unstable to an increasingly wide band of wave numbers. Similar striking differences in linear stability characteristics have been reported in the impulsively heated plate problems.[10]

As the two impulsively started flows have quite distinctive linear stability properties it is to be expected that there will be significant differences in the nature of the resulting nonlinear vortex motion. In particular, our main result is the determination of the structure of strongly nonlinear vortices in the impulsive shear case, finding an exact solution to the governing equations at large times. Unfortunately, for the impulsively started flow, we cannot justify, on mathematical or practical grounds, the standard analytical methods for obtaining weakly nonlinear solutions and only linear stability results are presented. Despite the limitations of our results for the impulsively started flow, this problem is used to introduce the scaling and WKB solution methods used for both the unsteady flows studied here.

We begin by considering axisymmetric motion in an incompressible fluid, of kinematic viscosity ν, generated by the rotation of a long circular cylinder of radius R. Initially the cylinder and surrounding fluid are at rest and at time $t^*=0$ the cylinder impulsively commences rotation about its longitudinal axis with angular velocity Ω. Thus the physical data defining the problem are ν, Ω, R, and ρ, the fluid density. From these constants a Reynolds number can be defined as $\mathrm{Re}=\Omega R^2/\nu$ and the fluid density can be removed from the problem by suitable scaling of the pressure.

Relative to the usual (r^*,θ^*,z^*) cylindrical polar coordinate system, scaled co-ordinates η and z and time t defined by

$$r^*=R+\eta d, \quad z^*=zd, \quad t^*=(d^2/\nu)t, \tag{1}$$

are introduced. Here d is some distance, to be defined in terms of the existing problem constants ν, Ω, and R only, and to be chosen so that the usual limit of large Re leaves centripetal pressure terms in the radial momentum equation and, simultaneously, allows the neglect of the term ηd compared to R. (This last geometrical simplification is often called the narrow gap approximation in the standard Taylor vortex problem.[11]) The velocity components of the fluid in the r^*, θ^*, and z^* directions together with the fluid pressure p^* are written as

$$\mathbf{u}^*=\left(\frac{\nu}{d}u,\Omega R v,\frac{\nu}{d}w\right), \quad p^*=\frac{\rho\nu^2}{d^2}p, \tag{2}$$

and with this scaling the required form of the governing equations can be obtained via the choice

$$d^3=\nu^2/\Omega^2 R, \tag{3}$$

so that $d=\mathrm{Re}^{-2/3}R$. The simplification of the geometry occurs as long as $\eta\,\mathrm{Re}^{-2/3}\ll 1$ or, as the extent of the developing Rayleigh layer is proportional to $t^{1/2}$, for times $t\ll\mathrm{Re}^{4/3}$. Assuming this holds, the governing Navier–Stokes and continuity equations for axisymmetric flow reduce to

$$\frac{\partial u}{\partial t}+u\frac{\partial u}{\partial\eta}+w\frac{\partial u}{\partial z}-v^2=-\frac{\partial p}{\partial\eta}+\nabla^2 u, \tag{4a}$$

$$\frac{\partial v}{\partial t}+u\frac{\partial v}{\partial\eta}+w\frac{\partial v}{\partial z}=\nabla^2 v, \tag{4b}$$

$$\frac{\partial w}{\partial t}+u\frac{\partial w}{\partial\eta}+w\frac{\partial w}{\partial z}=-\frac{\partial p}{\partial z}+\nabla^2 w, \tag{4c}$$

$$\frac{\partial u}{\partial\eta}+\frac{\partial w}{\partial z}=0, \tag{4d}$$

where $\nabla^2\equiv\partial^2/\partial\eta^2+\partial^2/\partial z^2$. These equations need to be supplemented by no-slip boundary conditions $u=w=0$, $v=1$ on $\eta=0$ (for $t\geqslant 0$), far-field decay u, v, $w\to 0$ as $\eta\to\infty$ and no motion $u=v=w\equiv 0$ prior to the initiation of the flow at time $t=0$.

II. THE LINEAR STABILITY OF IMPULSIVELY STARTED ROTATION

Equations (4) together with the associated boundary and initial conditions have the familiar Rayleigh layer solution for the basic flow

$$u=w=0, \quad v=\overline{V}(\eta,t)=\frac{2}{\sqrt{\pi}}\int_{\eta/\sqrt{4t}}^{\infty}\mathrm{e}^{-s^2}\,\mathrm{d}s,$$

$$p=\overline{p}=\int_{\eta}^{\infty}\overline{V}^2(\xi,t)\,\mathrm{d}\xi. \tag{5}$$

To examine the linear stability of this flow we set $\mathbf{u}=(0,\overline{V},0)+\delta(u,v,w)$ and $p\to\overline{p}+p\,\delta$, with $\delta\ll 1$, and linearize the equations to obtain

$$\frac{\partial u}{\partial t}-2\overline{V}v=-\frac{\partial p}{\partial\eta}+\nabla^2 u, \tag{6a}$$

$$\frac{\partial v}{\partial t}+u\frac{\partial\overline{V}}{\partial\eta}=\nabla^2 v, \tag{6b}$$

$$\frac{\partial w}{\partial t}=-\frac{\partial p}{\partial z}+\nabla^2 w, \tag{6c}$$

$$\frac{\partial u}{\partial\eta}+\frac{\partial w}{\partial z}=0. \tag{6d}$$

The standard quasi-steady approach is to *a priori* assume that disturbance growth rates are much larger than the time rate of change of the basic flow. Then, under this assumption, the equations governing the quasi-steady neutrally stable modes are

$$\left(\frac{\partial^2}{\partial\eta^2}-a^2\right)^2 u-2a^2\overline{V}v=0,$$

$$\left(\frac{\partial^2}{\partial\eta^2}-a^2\right)v-\frac{\partial\overline{V}}{\partial\eta}u=0, \tag{7}$$

where the disturbance has been taken to be periodic in the axial direction with wavelength $2\pi/a$.

The above equations contain two apparently contradictory ingredients: First that the growth rate of the distur-

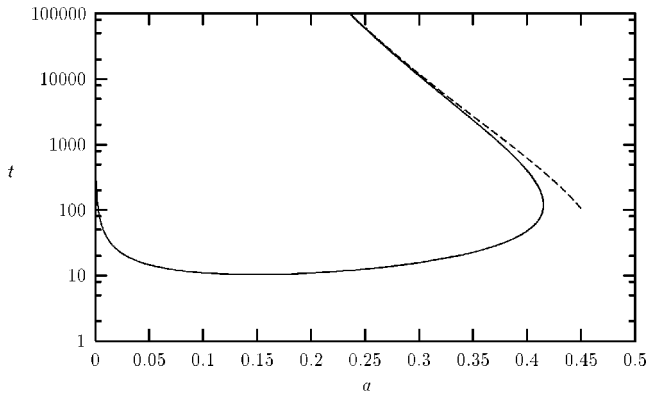

FIG. 1. Linear neutral stability curve for the impulsively started rotation problem, obtained by solving system (7) with base flow $\overline{V}$ given by (5). Shown dashed is the two-term small wave number asymptote (12).

bances is large (the quasi-steady ansatz) and second that the growth rate of the disturbances is zero (the marginal stability condition).[12] It is one of the aims of this paper to show that these conflicting conditions *can* lead to results which have a rigorous mathematical justification. When quasi-steady theory is inapplicable, energy-stability theory provides an alternative approach and this technique has been employed in a range of other papers[13–15] concerned with both centrifugal and thermal instabilities.

Unfortunately, the WKB techniques employed to justify the use of (7) are unable to validate the quasi-steady neutral curve at the critical conditions and hence large differences between theory and experiments determining the onset of instability are to be expected for the problems considered here. On the other hand, when quasi-steady theory can be rationalised, it does capture many other features of the stability problem and it is these aspects that we concentrate upon.

Equations (7) need to be solved subject to the no-slip and far-field conditions $u=\partial u/\partial\eta=v=0$ at $\eta=0$ and as $\eta\to\infty$. The time t appears in these equations only as a parameter and the quasi-steady neutral curve, t versus a, obtained by a numerical solution of (7) is given in Fig. 1. The neutral curve for this centrifugal instability does not have the usual shape associated with Taylor or Görtler vortex problems[16] and instead clearly shows that the basic flow is always linearly stable to disturbances with (dimensional) wavelengths smaller than approximately $4\pi\,\mathrm{Re}^{-2/3}R$. Such a conclusion is not easily extracted from the quasi-steady neutral curve given in Otto,[8] where the characteristic length scale for the Taylor number is taken as the "Rayleigh layer thickness," $\sqrt{\nu t}$.

Also shown in Fig. 1 is the result of a WKB analysis, based on the limit of $t\to\infty$, of the full time-dependent problem (6). This is the only section of the "neutral curve" where the quasi-steady assumption is valid, as on all other parts the disturbances and the basic flow are changing on the same time scale. In these regions the evolution of disturbances to the basic state is governed by parabolic equations and numerical methods are needed to locate the true neutral curve.[5] However, it can be shown[10] that for t larger than $O(a^{-4/5})$ and above the lower part of this "neutral curve," the quasi-steady assumption does hold and the modal structure of the disturbances can be determined as $a\to 0$.

Along the upper branch of the neutral curve the vortex activity is concentrated in a relatively thin layer on the surface of the cylinder. This velocity field is analogous to that described by Hall[16] for large wave number vortices in the steady Taylor vortex problem, and so similar balances are sought in the governing equations. Requiring $\overline{V}|_0 v$ to balance a^2u in the radial momentum equation and $\partial\overline{V}/\partial\eta|_0 u \sim a^2 v$ in the azimuthal equation gives the asymptote $t\sim O(a^{-8})$ as $a\to 0$ for the neutral curve. More detailed analysis shows that the region of vortex activity is $O(a^{-2})$ thick, compared to the Rayleigh layer depth of $O(a^{-4})$, as $a\to 0$, and so the region of vortex activity is small compared to the Rayleigh layer thickness. Thus, WKB solutions to the full time-dependent equations (6) are sought in the form

$$(u,v,w,p)=(\hat{u}(\tau,Y)\cos az,\hat{v}(\tau,Y)\times\cos az,\hat{w}(\tau,Y)\sin az,\hat{p}(\tau,Y)\cos az),$$

with

$$(\hat{u},\hat{v},\hat{w},\hat{p})=(U_0+a^2U_2+\cdots,a^2V_0+a^4V_2+\cdots,aW_0+a^3W_2+\cdots,a^2P_0+a^4P_2+\cdots)\times\exp[a^{-6}(g_0(\tau)+a^2g_2(\tau)+\cdots)],\qquad(8)$$

where $\tau=a^8t$ and $Y=a^2\eta$ and where the unknown functions $U_i,V_i,\ldots$ depend on τ and Y. The leading order approximations to Eqs. (6) are then

$$(1+g_0')U_0=2V_0,$$
$$(1+g_0')V_0=U_0/\sqrt{\pi\tau},\qquad(9)$$

and hence $(1+g_0')^2=2/\sqrt{\pi\tau}$. To leading order, the disturbances are neutrally stable when $g_0'=0$ and hence we obtain the leading order asymptote $t\sim 4a^{-8}/\pi$ for the upper branch of the neutral curve.

The next order approximations from Eq. (6) determine the structure of the velocity field and the correction to the growth rate. The governing equation becomes

$$\frac{\partial^2U_0}{\partial Y^2}-\frac{1}{(3+g_0')}\left(\frac{1+g_0'}{\sqrt{\pi\tau}}Y+2g_2'\right)U_0=0,\qquad(10)$$

subject to $U_0=\partial U_0/\partial Y=0$ at $Y=0$ and $U_0\to 0$ as $Y\to\infty$. A satisfactory solution can only be obtained by dropping the derivative condition on U_0, and in this case, U_0 becomes a multiple of the Airy function Ai and the growth rate correction is given by

$$g_2'=2^{-2/3}(\pi\tau)^{-1/2}(2+\sqrt{2}(\pi\tau)^{-1/4})^{1/3}\zeta_0.\qquad(11)$$

Here $\zeta_0\approx -2.3381\cdots$ is the first zero of $\mathrm{Ai}(\zeta)$. A wall layer of thickness $O(a^{-1})$ is needed in order to re-impose the derivative condition on U_0, but this layer can be shown to be passive and to have no effect on the growth rates at this order.

A two-term approximation to the neutral curve can be obtained by requiring that the growth rate vanish, i.e., requiring $g_0'+a^2g_2'=0$. This condition leads to the result $\tau=4[1+6^{1/3}\zeta_0 a^2+\cdots]/\pi$, or, in terms of t

$$t_n=\frac{4a^{-8}}{\pi}[1+6^{1/3}\zeta_0 a^2+\cdots], \tag{12}$$

which is the asymptote plotted on Fig. 1. It is possible to find WKB solutions for the essentially inviscid, rapidly growing vortices in the parameter range $O(a^{-4/5})<t<t_n$ as $a\to 0$, but as the actual initiation of the vortex motion is governed by the full parabolic system (6) these modal calculations would have little practical relevance. The main result of the calculations presented so far is the unusual nature of the quasi-steady neutral curve as $t\to\infty$ and its justification by a rational, asymptotic WKB approach. A different form for the linear stability neutral curve is obtained in the impulsive shear case, which is given in the next section.

III. THE IMPULSIVE SHEAR PROBLEM

To contrast with the situation of the impulsively started cylinder, we now examine the flow generated when the speed of the surface of the cylinder is $k(t^*)^{1/2}$ where t^* is the dimensional time and k is a given $O(1)$ constant. In this case the initiation of the flow is less abrupt than in the impulsively started flow, and the form of the time dependence of the angular velocity leads to a basic undisturbed flow with a constant wall shear stress. Before proceeding further, the nondimensionalization employed in Eq. (2) above needs to be modified as there is no longer an explicit *constant* angular velocity scale imposed on the flow. Noting that $k/\sqrt{\nu}$ has the same units as angular velocity, the form for the azimuthal velocity v^* is now taken to be $v^*=(kd/\sqrt{\nu})v$ [cf. (2)] so that the value of d is now

$$d=R(\nu^3/R^4k^2)^{1/5}=R\,\mathrm{Re}^{-2/5}. \tag{13}$$

The resulting system of governing equations is precisely (4) again, but the no-slip conditions to be imposed on $\eta=0$ are now $u=w=0$ and $v=t^{1/2}$. As shown below in (14), the viscous layer on the cylinder, in the undisturbed flow, has a thickness proportional to $t^{1/2}$, so that the requirement for the ''small-gap'' approximation to be valid is now $t\ll\mathrm{Re}^{4/5}$. However, the results of the strongly nonlinear calculations in Sec. III B indicate that the thickness of the layer on the cylinder grows much faster than $t^{1/2}$, and hence a more stringent condition on t is needed for the neglect of the curvature terms to remain valid. The details are presented at the end of Sec. III B.

The basic flow solution is given by

$$v=\overline{V}(\eta,t)=t^{1/2}f(\eta/\sqrt{t}),$$

$$f(\phi)=\mathrm{e}^{-\phi^2/4}-\phi\int_{\phi/2}^{\infty}\mathrm{e}^{-s^2}\,\mathrm{d}s, \tag{14}$$

and the natural starting point for a stability analysis of this flow is the quasi-steady linearized equations (7). The corresponding neutral stability curve, in the a-t plane, obtained via a numerical solution of (7) is shown in Fig. 2. Here we

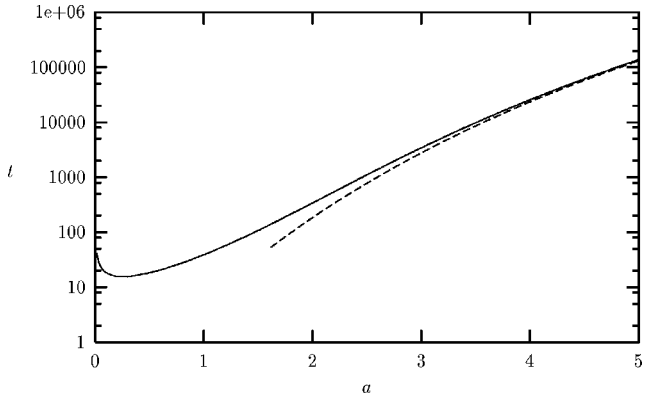

FIG. 2. Linear neutral stability curve for the impulsive shear problem, obtained by solving system (7) with base flow $\overline{V}$ given by (14). Shown dashed is the two-term large wave number asymptote (19).

see that the current basic flow is linearly unstable to all wave numbers and that the neutral curve has an asymptote with $t\to\infty$ as $a\to\infty$. These properties are in marked contrast to the neutral curve obtained in the impulsively started flow (cf. Fig. 1). As previously, the large time asymptote of the neutral curve can be derived analytically via WKB methods, but now the appropriate rescaling of time is given by $t=a^8\tau$ as $a\to\infty$. With this form for t, and basic flow $\overline{V}$ given by (14), simple balances within (6) show that the vortex activity is now confined to the region where $\eta=a^{2/3}Y$. The WKB solution has the form

$$(u,v,w,p)=(\hat{u}(\tau,Y)\cos az,\hat{v}(\tau,Y)\times\cos az,\hat{w}(\tau,Y)\sin az,\hat{p}(\tau,Y)\cos az),$$

with

$$\begin{aligned}(\hat{u},\hat{v},\hat{w},\hat{p})=(&U_0+a^{-10/3}U_1+\cdots,a^{-2}V_0+a^{-16/3}V_1\\&+\cdots,a^{-5/3}W_0+a^{-5}W_1+\cdots,a^{-2/3}P_0\\&+a^{-4}P_1+\cdots)\exp[a^{10}(g_0(\tau)\\&+a^{-20/3}g_1(\tau)+\cdots)],\end{aligned} \tag{15}$$

where each unknown is a function of τ and Y. The substitution of (15) in (6a) and (6b) shows that U_0 and V_0 are governed by

$$\begin{aligned}&(1+g_0')U_0=2\tau^{1/2}V_0,\\&(1+g_0')V_0=\frac{1}{2}\sqrt{\pi}U_0,\end{aligned} \tag{16}$$

and the consistency of these two equations requires $(1+g_0')^2=\sqrt{\pi\tau}$.

The details of the vortex structure are found by obtaining the equations coupling U_1 and V_1. The compatibility requirement for these two nonhomogeneous equations reduces to the satisfaction of

$$\frac{\partial^2U_0}{\partial Y^2}-\frac{(\pi+2)}{2(3+g_0')(1+g_0')}YU_0-\frac{2g_1'}{3+g_0'}U_0=0, \tag{17}$$

subject to the boundary conditions $U_0 = \partial U_0/\partial Y = 0$ at $Y = 0$ and $U_0 \to 0$ as $Y \to \infty$. The solution for U_0 follows the path outlined in Sec. II for dealing with (10): U_0 is a multiple of Ai; g_1' is given by

$$g_1' = 2^{-5/3}\zeta_0(\pi+2)^{2/3}(\pi\tau)^{-1/12}[1+2(\pi\tau)^{-1/4}]^{1/3}, \tag{18}$$

where ζ_0 is a zero of the Airy function Ai; and the details of a passive wall-layer have been ignored.

The large-a asymptote for the neutral stability curve

$$t = a^8\pi^{-1} - 6^{1/3}(\pi+2)^{2/3}\zeta_0 a^{14/3}/\pi + \cdots, \tag{19}$$

is superimposed on Fig. 2 which shows that the analytical and numerical solutions are in very good agreement in this limit. The overall form of this neutral curve indicates that the critical conditions for the initiation of vortex motion are likely to be near $a = 0.25$ and $\tau = 5.4$. These conditions are well away from the region where current analytical techniques for Eqs. (6) can be justified mathematically and so numerical methods would be needed to locate the commencement of vortex motion and its subsequent nonlinear development with time. However, for monochromatic disturbances with large wave numbers, existing analytical methods can be applied to determine the structure and time-development of the vortex motion. Further, as the flow does not evolve through a region governed by parabolic equations, as was the case in Sec. II, these solutions can be justified mathematically. Clearly, any large wave number solution has little relevance to the critical conditions for instability, but these large a solutions will provide useful checks for any completely numerical attack on the problem.

A. Weakly nonlinear solutions

The above analysis of the right-hand portion of the neutral stability curve can be extended to study nonlinear vortex motion. In order to proceed to fully nonlinear vortices however, it is first necessary to investigate the properties of the weakly nonlinear modes whose structure follows on from the above linear theory results. Thus the disturbance is concentrated in a $\eta = O(a^{2/3})$ region attached to the surface of the cylinder so that for $a \gg 1$ the relevant time and length scales are

$$t = a^8\tau_0 + a^{14/3}\hat{t}, \quad (\tau_0 = \pi^{-1}) \quad \eta = a^{2/3}Y, \tag{20}$$

where $\hat{t}$ is the appropriate temporal scale over which the weakly nonlinear vortices will develop. With these choices the basic flow expands as

$$\overline{V} = a^4\tau_0^{1/2} + \left(\frac{\hat{t}}{2\sqrt{\tau_0}} - \frac{1}{2}\sqrt{\pi}Y\right)a^{2/3} + \frac{(2\tau_0 Y^2 - \hat{t}^2)}{8\tau_0^{3/2}}a^{-8/3} + \cdots, \tag{21a}$$

$$\frac{\partial \overline{V}}{\partial \eta} = -\frac{1}{2}\sqrt{\pi} + \frac{Y}{2\sqrt{\tau_0}}a^{-10/3} + \cdots. \tag{21b}$$

The flow field needs to be decomposed as

$$(u,v,w,p) = (0,\overline{V},0,\overline{p}) + (U,V,W,P), \tag{22}$$

where the quantities with an overbar denote the basic flow values while U, V, W, and P are the components of the disturbance. The governing system (4) may be rewritten as

$$\frac{\partial U}{\partial t} - 2\overline{V}V + \frac{\partial P}{\partial \eta} - \frac{\partial^2 U}{\partial \eta^2} - \frac{\partial^2 U}{\partial z^2} = -U\frac{\partial U}{\partial \eta} - W\frac{\partial U}{\partial z} + V^2, \tag{23a}$$

$$\frac{\partial V}{\partial t} + \frac{\partial \overline{V}}{\partial \eta}U - \frac{\partial^2 V}{\partial \eta^2} - \frac{\partial^2 V}{\partial z^2} = -U\frac{\partial V}{\partial \eta} - W\frac{\partial V}{\partial z}, \tag{23b}$$

$$\frac{\partial W}{\partial t} + \frac{\partial P}{\partial z} - \frac{\partial^2 W}{\partial \eta^2} - \frac{\partial^2 W}{\partial z^2} = -U\frac{\partial W}{\partial \eta} - W\frac{\partial W}{\partial z}, \tag{23c}$$

$$\frac{\partial U}{\partial \eta} + \frac{\partial W}{\partial z} = 0, \tag{23d}$$

so that terms on the left-hand sides of these balances are linear in the disturbance quantities while those on the right are nonlinear. Solutions are sought in the form

$$U = a^{-2/3}(U_{10} + a^{-10/3}U_{11} + \cdots)\cos az + a^{-4}(U_{20} + \cdots)\cos 2az + \cdots, \tag{24a}$$

$$V = a^{-8/3}V_M + \cdots + a^{-8/3}(V_{10} + a^{-10/3}V_{11} + \cdots)\cos az + a^{-6}(V_{20} + \cdots)\cos 2az + \cdots, \tag{24b}$$

$$W = a^{-7/3}(W_{10} + a^{-10/3}W_{11} + \cdots)\sin az + a^{-17/3}(W_{20} + \cdots)\sin 2az + \cdots, \tag{24c}$$

$$P = a^2 P_M + \cdots + a^{-4/3}(P_{10} + a^{-10/3}P_{11} + \cdots)\cos az + a^{-14/3}(P_{20} + \cdots)\cos 2az + \cdots, \tag{24d}$$

where the unknowns are functions of Y and $\hat{t}$. The substitution of (24) into (23) gives the leading-order fundamental equations

$$-2\sqrt{\tau_0}V_{10} + U_{10} = 0, \quad -\frac{1}{2}\sqrt{\pi}U_{10} + V_{10} = 0,$$

$$P_{10} = W_{10}, \quad W_{10} = -\frac{\partial U_{10}}{\partial Y}. \tag{25}$$

The first two of these are consistent only if $\tau_0 = \pi^{-1}$, agreeing with the underlying linear theory, while the details of the spatial structure of the vortex motion requires consideration of the next order terms. The consistency of the equations

$$-2\sqrt{\tau_0}V_{11} + U_{11} = \sqrt{\pi}(\hat{t} - Y)V_{10} + \frac{\partial^2 U_{10}}{\partial Y^2} - \frac{\partial P_{10}}{\partial Y}, \tag{26a}$$

$$-\frac{1}{2}\sqrt{\pi}U_{11} + V_{11} = -\frac{Y}{2\sqrt{\tau_0}}U_{10} + \frac{\partial^2 V_{10}}{\partial Y^2} - U_{10}\frac{\partial V_M}{\partial Y}, \tag{26b}$$

gives the condition governing U_{10} as

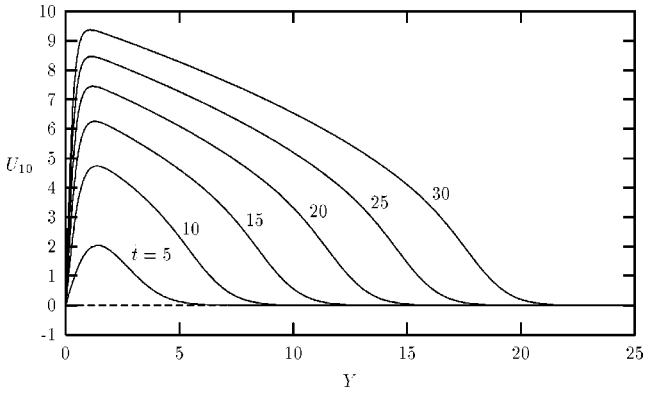

FIG. 3. Structure of the vortex velocity component $U_{10}(Y)$ determined from Eqs. (27) and (28) for various scaled times: $\hat{t}=5$, 10, 15, 20, 25, and 30.

$$3\frac{\partial^2 U_{10}}{\partial Y^2}-\frac{1}{2}[(\pi+2)Y-\pi\hat{t}]U_{10}-\frac{2}{\sqrt{\pi}}U_{10}\frac{\partial V_M}{\partial Y}=0. \tag{27}$$

The equation for the mean flow term, V_M, is obtained from the azimuthal momentum equation (23b) and is

$$\frac{\partial V_M}{\partial Y}=\frac{1}{4}\sqrt{\pi}U_{10}^2. \tag{28}$$

The coupled system needs to be solved subject to the requirements that $U_{10}=V_M=0$ at the wall $Y=0$ and that the vortex quantity $U_{10}\to 0$ as $Y\to\infty$. Some typical numerical solutions of (27), (28) for various values of the parameter $\hat{t}$ are shown in Fig. 3. Analogous results have also been obtained for weakly nonlinear vortex motion on an oscillating cylinder.[19] These numerical results show that the vortex is confined to a zone, next to the cylinder surface $Y=0$, which grows with $\hat{t}$. In fact an asymptotic solution of (27) and (28) for large $\hat{t}$ can be found. To do this we rescale $Y=\hat{t}\,\hat{y}$ and make the ansatz that in the main core region $U_{10}=\hat{t}^{1/2}\hat{U}_{10}$ and $V_M=\hat{t}^2\hat{V}_M$. At leading order equation (27) becomes

$$\hat{U}_{10}^2=\pi-(\pi+2)\hat{y}, \tag{29}$$

which vanishes at $\hat{y}=\pi/(\pi+2)$. Of course this solution does not fulfill the wall-condition that $U_{10}=0$ on $Y=0$ and this requirement suggests that a thin layer must develop there. Within this zone $Y=\hat{t}^{-1/2}\tilde{Y}$ and $U_{10}=\hat{t}^{1/2}\tilde{U}_{10}$ where

$$3\frac{\partial^2\tilde{U}_{10}}{\partial\tilde{Y}^2}+\frac{1}{2}\pi\tilde{U}_{10}-\frac{1}{2}\tilde{U}_{10}^3=0, \tag{30}$$

this equation has the solution $\tilde{U}_{10}=\sqrt{\pi}\tanh(\tilde{Y}\sqrt{\pi/12})$ which satisfies $\tilde{U}_{10}=0$ at $\tilde{Y}=0$ and matches with the core solution (29) as $\tilde{Y}\to\infty$.

The form of (29) as $\hat{y}\to\pi/(\pi+2)$ indicates that the vortex amplitude develops a square-root form around this point. In order to smooth this behavior it is necessary to introduce a scaled co-ordinate $\bar{y}=O(1)$ so $Y=\pi\hat{t}/(\pi+2)+\bar{y}$. The system (27), (28) then reduces to

$$3\frac{d^2U_{10}}{d\bar{y}^2}-\frac{1}{2}(\pi+2)\bar{y}U_{10}-\frac{1}{2}U_{10}^3=0, \tag{31}$$

an equation which is effectively the second Painlevé transcendent. Hastings and McLeod[17] have proved rigorously that this equation admits a solution for which U_{10} grows in a square-root manner as $\bar{y}\to-\infty$ [and thereby matching with the core solution (29)] while decaying exponentially as $\bar{y}\to\infty$. The result is that above $Y=\pi\hat{t}/(\pi+2)$ the vortex motion is completely extinguished and all that remains is a residual azimuthal mean-flow adjustment—this remnant is brought to zero through a diffusion layer of depth $O(a^{7/3}\hat{t}^{1/2})$.

The crucial result of this large time analysis is that the correction to the azimuthal mean flow attains the size $O(a^{-8/3}\hat{t}^2)$ in a region of thickness $O(a^{2/3}\hat{t})$. From (21a) the undisturbed flow has an $O(a^4)$ azimuthal velocity, which is comparable to the mean flow correction when $\hat{t}\sim O(a^{10/3})$. At these large times the thickness of both the vortex activity region and the diffusion layer has expanded to $O(a^4)$, which is the same as the undisturbed Rayleigh layer thickness, indicating that the vortex motion is so intense that it leads to a zeroth-order change to the underlying mean flow.

B. Strongly nonlinear vortex motion

The details of a strongly nonlinear flow follow from the asymptotic solutions outlined above. The bulk of the activity is to be found in the region where $\eta=O(a^4)$ and appropriate temporal and spatial scales are defined by

$$t=a^8\tau,\quad \eta=a^4\phi. \tag{32}$$

Solutions of the full nonlinear equations (4) are sought in the form

$$u=a(U_{10}+a^{-4}U_{11}+\cdots)\cos az+a^{-4}(U_{20}+\cdots)\cos 2az+\cdots, \tag{33a}$$

$$v=a^4\bar{v}_0+\bar{v}_1+\cdots+a^{-1}(V_{10}+a^{-4}V_{11}+\cdots)\cos az+a^{-6}(V_{20}+\cdots)\cos 2az+\cdots, \tag{33b}$$

$$w=a^{-4}(W_{10}+a^{-4}W_{11}+\cdots)\sin az+a^{-9}(W_{20}+\cdots)\sin 2az+\cdots, \tag{33c}$$

$$p=a^{12}\bar{p}_0+a^8\bar{p}_1+\cdots+a^{-3}(P_{10}+a^{-4}P_{11}+\cdots)\cos az+a^{-8}(P_{20}+\cdots)\cos 2az+\cdots, \tag{33d}$$

where all the unknowns are functions of ϕ and τ. To the orders that are required here the higher harmonics are unimportant and, as is characteristic of strongly nonlinear flows of this type, a consistency condition on the leading-order vortex equations will determine the mean flow. The substitution of (33) in (4) leads to

$$-2\bar{v}_0V_{10}=-U_{10},\quad U_{10}\frac{\partial\bar{v}_0}{\partial\phi}=-V_{10},$$

$$P_{10}=W_{10},\quad W_{10}=-\frac{\partial U_{10}}{\partial\phi}, \tag{34}$$

so that for consistency we require

$$2\bar{v}_0\frac{\partial\bar{v}_0}{\partial\phi}=-1 \quad \text{or} \quad \bar{v}_0=\sqrt{b(\tau)-\phi}, \tag{35}$$

for some function $b(\tau)$. The leading-order mean flow components of the azimuthal momentum equation (4b), together with the results (34), give the equation

$$\frac{\partial^2\bar{v}_0}{\partial\phi^2}-\frac{\partial\bar{v}_0}{\partial\tau}=-\frac{1}{2}\frac{\partial}{\partial\phi}\left[\frac{\partial\bar{v}_0}{\partial\phi}U_{10}^2\right], \tag{36}$$

which determines the fundamental component, U_{10}, of the vortex. If the outer edge of the vortex is located at $\phi=\phi_1(\tau)$, one integration of (36) and the requirement that $U_{10}\to 0$ as $\phi\to\phi_1$ combine to show

$$U_{10}^2=\sqrt{\frac{b-\phi}{b-\phi_1}}[2-4b'(\tau)(b-\phi_1)] +4b'(\tau)(b(\tau)-\phi)-2. \tag{37}$$

This result demonstrates that $U_{10}\to 0$ algebraically as $\phi\to\phi_1$ and to explain the form of the disturbance around $\phi=\phi_1$ it is necessary to examine the flow characteristics in a thin region centred there. The manipulations required were first performed by Hall and Lakin[18] for nonlinear Görtler vortices and since then numerous papers have described similar calculations in a variety of related contexts.[19–21] For the sake of brevity we do not repeat the details here but rather summarize the situation by noting that in the vicinity of $\phi=\phi_1$ the square-root behavior of U_{10} is transformed to an exponential decay for $\phi>\phi_1$ [and this occurs through the solution of a scaled form of the second Painlevé transcendent, cf. (31)]. The result is that for $\phi>\phi_1$ the vortex is completely destroyed and all that remains is an azimuthal mean velocity field. From (36) this flow satisfies

$$\frac{\partial^2\bar{v}_0}{\partial\phi^2}=\frac{\partial\bar{v}_0}{\partial\tau}, \tag{38}$$

and it is easy to demonstrate that both the mean flow, $\bar{v}_0$, and its spatial derivative must be continuous across $\phi=\phi_1$. The use of (35) shows that (38) must be solved in $\phi>\phi_1(\tau)$ subject to decay as $\phi\to\infty$ and

$$\bar{v}_0=\sqrt{b(\tau)-\phi_1}, \qquad \frac{\partial\bar{v}_0}{\partial\phi}=-\frac{1}{2\sqrt{b(\tau)-\phi_1}} \quad \text{at} \quad \phi=\phi_1. \tag{39}$$

The overall flow structure is now almost complete but to finish it is necessary to consider the form of $b(\tau)$. It has been seen how nonlinear motions are located in the region $0\leqslant\phi\leqslant\phi_1(\tau)$ and in order that the mean flow in this zone match with the velocity of the cylinder on $\phi=0$ it is evident from (35) that $b(\tau)=\tau$. With this choice however, the form of (37) suggests that the vortex activity does not vanish at $\phi=0$ contrary to the required constraints. To resolve this a thin layer at $\phi=0$ is introduced in which the necessary decay can take place. This layer turns out to have depth $\phi=O(a^{-5})$ [or $\eta=O(a^{-1})$ from (32)] and since this is comparable to the dimensionless wavelength of the vortex, all the harmonics of the vortex are of the same order of magnitude here. This leads to a coupled set of infinitely many ordinary differential equations. Similar systems have been derived in other contexts; for example, in curved channel flows,[20] for Taylor vortices,[21] for short wavelength Bénard convection[22] and for curved Stokes layer flows.[23] In the present problem this wall layer is passive and we do not need to determine its structure.

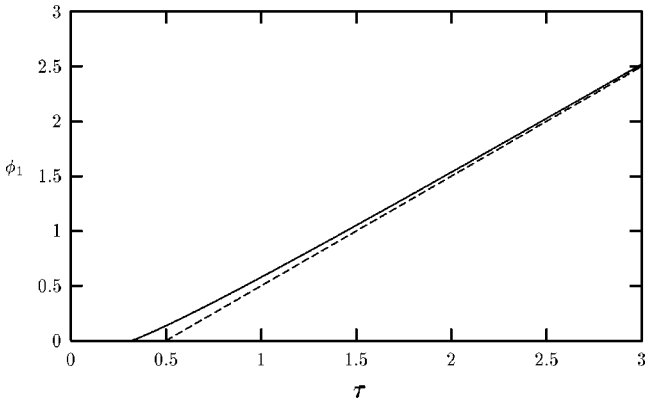

FIG. 4. Solution of the free-boundary value problem (38) subject to (39) and the requirements $b(\tau)=\tau$ and $\bar{v}_0\to 0$ as $\phi\to\infty$. Shown is the position of the outer extent of the vortex activity, $\phi_1(\tau)$ obtained via a numerical solution. The large-τ asymptote $\phi_1(\tau)\sim\tau-\frac{1}{2}$ [see (40)] is shown dashed.

The problem that remains to be solved to complete the determination of this strongly nonlinear vortex motion is the free boundary value system (38) subject to (39) with $b(\tau)=\tau$ and $\bar{v}_0\to 0$ as $\phi\to\infty$. The weakly nonlinear theory described previously shows that motion will commence when the scaled time $\tau=\pi^{-1}$ [see (20)], and following the methods used in Horseman *et al.*,[19] suitable initial conditions can be derived to complete the specification of the system. The resulting numerical solution for $\phi_1(\tau)$, obtained using the NAG routine D03PHF, is shown in Fig. 4. The unexpected result from this numerical solution is that ϕ_1 grows almost linearly with τ, especially for large τ. This result is perhaps less surprising when it is recognized that (38) and (39) admit the exact analytical solution

$$\bar{v}_0=\frac{1}{\sqrt{2}}e^{\tau-\phi-(1/2)} \quad \text{with} \quad \phi_1=\tau-(1/2). \tag{40}$$

Thus, during a short period of time after $\tau=\pi^{-1}$ the solution relaxes from the given initial conditions to this simple exponential profile and the extent of domain of vortex activity grows like τ. This result shows the effectiveness of the vortex motion in transferring momentum away from the cylinder wall as the viscous diffusion mechanisms present in the undisturbed flow only allow the boundary layer thickness to grow like $t^{1/2}$. The rapid growth of the strongly nonlinear vortex region also imposes more severe restrictions on the applicability of the ''small gap'' limit taken at the beginning of this analysis. Due to the linear growth in time of the boundary layer thickness, we now need $t\ll\mathrm{Re}^{2/5}$ so that the approximation of the cylindrical polar form of the governing equations by an essentially Cartesian form is valid. (It has kindly been pointed out to us that as the limiting times for our analysis are functions of the Reynolds number, an

alternative way to view these constraints is that our arguments are valid only for Reynolds numbers exceeding certain values which can be inferred from the critical times predicted in Figs. 1 and 2. Of course, these in turn depend upon the disturbance wave number.)

IV. CONCLUDING REMARKS

Under the global scaling used here the linear theory neutral stability curves, Figs. 1 and 2, for the two impulsively generated flows examined have striking differences. The large-time behavior of the asymptotes for each neutral curve are

$a \sim t^{-1/8}$ impulsive velocity change,

$a \sim t^{1/8}$ impulsive wall shear change,

as $t \to \infty$. These behaviors can also be compared to the properties of the linear theory neutral curves obtained for the related unsteady thermal boundary layers.[10] Using a similar global scaling, the asymptotes of the neutral curves in the thermal problems are

$a \sim t^{-1/8}$ impulsive temperature change,

$a \sim 1$ impulsive heat flux change,

as $t \to \infty$. For the step change in the velocity or the temperature, it is not surprising that the basic state becomes more stable as time becomes large, as in both of these cases the gradients of the basic velocity or temperature are decaying to zero with increasing time. We know of no simple explanation for the difference between the remaining two cases. These linear theory differences lead to contrasts in the strongly nonlinear solutions available: For the thermal problem, strongly nonlinear vortex motion solutions can be found for any wave number $0 < a < 1$ as $t \to \infty$, while in the current rotating cylinder problem we need $a \to \infty$ as well. However for both strongly nonlinear solutions, the extent of the vortex region grows linearly with time.

Although not strictly valid, it is useful to compare the ''neutral stability'' predictions for the impulsively started cylinder with existing experimental results.[1] As the analysis here has assumed the limit $\mathrm{Re} \to \infty$, direct comparison with experiment is awkward, but selecting those experimental runs with the largest value of Reynolds number, $\mathrm{Re} = 275$, and transforming to the scaling of this paper, the results of Kirchner and Chen[1] indicate a time to instability of $t \approx 79$; with $\mathrm{Re} = 30.8$ the corresponding time is $t \approx 222$. These results are to be compared with the calculations summarized in Fig. 1, which indicate the time to instability is given by $t \approx 10$. The difference between the assumption of an infinite fluid for the analysis here and the finite fluid annulus in the experiments is believed to be irrelevant as it was reported that the observed instability occurred well before the Rayleigh layer on the rotating cylinder had expanded to fill the gap between the cylinders. The results of Fig. 1 are in closer agreement with the related numerical calculations,[5] based on the numerical integration in time of the system (6), where, in our notation, a time to instability of $t \approx 34$ is reported for $200 \leqslant \mathrm{Re} \leqslant 400$. This is to be compared with the calculations of Liu and Chen[6] for the full nonlinear equations (4), where times to instability ranging from $t \approx 90$ to $t \approx 126$ are reported for $200 \leqslant \mathrm{Re} \leqslant 600$. As is well known, much of this variation can be ascribed to the experimental method or analytical criterion used to determine the critical conditions.

Finally, we point out that although the strongly nonlinear solutions of Sec. III are based on $a \to \infty$, the neutral curve in Fig. 2 suggests that large wave number asymptotic structures have set in for wave numbers as small as 4 or 5, and hence it is not unreasonable to use these analytical solutions to validate numerical codes designed to investigate vortex motion in unsteady flows.

ACKNOWLEDGMENTS

This investigation was conducted while S.O.M. and A.P.B. were visiting UNSW. They are indebted to the Australian Research Council without whose grants their visits would not have been possible.

[1] R. P. Kirchner and C. F. Chen, ''Stability of time-dependent rotational Couette flow. Part 1. Experimental investigation,'' J. Fluid Mech. **40**, 39 (1970).
[2] E. R. Cooper, D. F. Jankowski, G. P. Neitzel, and T. H. Squire, ''Experiments on the onset of instability in unsteady circular Couette flow,'' J. Fluid Mech. **161**, 97 (1985).
[3] Y. Takeda, K. Kobashi, and W. E. Fischer, ''Observation of the transient behaviour of Taylor vortex flow between rotating concentric cylinders after sudden start,'' Exp. Fluids **9**, 317 (1990).
[4] G. P. Neitzel, ''Marginal stability of impulsively initiated Couette flow and spin-decay,'' Phys. Fluids **25**, 226 (1982).
[5] C. F. Chen and R. P. Kirchner, ''Stability of time-dependent rotational Couette flow. Part 2. Stability analysis,'' J. Fluid Mech. **48**, 365 (1971).
[6] D. C. S. Liu and C. F. Chen, ''Numerical experiments on time-dependent rotational Couette flow,'' J. Fluid Mech. **59**, 77 (1973).
[7] G. P. Neitzel, ''Numerical computation of time-dependent Taylor-vortex flows in finite-length geometries,'' J. Fluid Mech. **141**, 51 (1984).
[8] S. R. Otto, ''Stability of the flow around a cylinder: The spin-up problem,'' IMA J. Appl. Math. **51**, 13 (1993).
[9] R. J. Goldstein and R. J. Volino, ''Onset and development of natural convection above a suddenly heated surface,'' Trans. ASME, J. Heat Transf. **117**, 808 (1995).
[10] A. P. Bassom and P. J. Blennerhassett, ''Impulsively generated convection in a semi-infinite fluid layer above a heated flat plate,'' Q. J. Mech. Appl. Math. **55**, 563 (2002).
[11] P. G. Drazin and W. H. Reid, *Hydrodynamic Stability* (Cambridge University Press, Cambridge, 1981).
[12] G. M. Homsy, ''Global stability of time-dependent flows: impulsively heated or cooled fluid layers,'' J. Fluid Mech. **60**, 129 (1973).
[13] R. J. Gumerman and G. M. Homsy, ''The stability of uniformly acclerated flows with application to convection driven by surface tension,'' J. Fluid Mech. **68**, 191 (1975).
[14] G. P. Neitzel, ''Stability of circular Couette flow with variable inner cylinder speed,'' J. Fluid Mech. **123**, 43 (1982).
[15] G. P. Neitzel, ''Onset of convection in impulsively heated or cooled fluid layers,'' Phys. Fluids **25**, 210 (1982).
[16] P. Hall, ''Taylor–Görtler vortices in fully developed or boundary-layer flows: linear theory,'' J. Fluid Mech. **124**, 475 (1982).
[17] S. P. Hastings and J. B. McLeod, ''A boundary value problem associated with the second Painlevé transcendent and the Korteweg–de Vries equation,'' Arch. Ration. Mech. Anal. **73**, 31 (1980).
[18] P. Hall and W. D. Lakin, ''The fully nonlinear development of Görtler vortices in growing boundary layers,'' Proc. R. Soc. London, Ser. A **415**, 421 (1988).
[19] N. J. Horseman, A. P. Bassom, and P. J. Blennerhassett, ''Strongly nonlinear vortices in the Stokes layer on an oscillating cylinder,'' Proc. R. Soc. London, Ser. A **452**, 1087 (1996).
[20] A. P. Bassom and P. J. Blennerhassett, ''The structure of highly nonlinear

vortices in curved channel flow,'' Proc. R. Soc. London, Ser. A **439**, 317 (1992).
[21]J. P. Denier, ''The structure of fully nonlinear Taylor vortices,'' IMA J. Appl. Math. **49**, 15 (1992).
[22]P. J. Blennerhassett and A. P. Bassom, ''Nonlinear high-wavenumber Bénard convection,'' IMA J. Appl. Math. **52**, 51 (1994).
[23]N. J. Horseman, ''Nonlinear instabilities in curved flows,'' Ph.D. thesis, University of Exeter, UK, 1991.